JACS
JOURNAL OF THE AMERICAN CHEMICAL SOCIETY
Article
pubs.acs.org/JACS

# Spontaneous Multielectron Transfer from the Surfaces of PbS Quantum Dots to Tetracyanoquinodimethane

Kathryn E. Knowles, Michał Malicki, Radha Parameswaran, Laura C. Cass, and Emily A. Weiss*

Department of Chemistry, Northwestern University, Evanston, Illinois 60208-3113, United States

Supporting Information

**ABSTRACT:** This paper describes an investigation of the interfacial chemistry that enables formation of a multielectron ground-state charge-transfer (CT) complex of oleate-coated PbS quantum dots (QDs) and tetracyanoquinodimethane (TCNQ) in $CHCl_3$ dispersions. Thermodynamically spontaneous electron transfer occurs from sulfur ions on the surfaces of the QDs (radius = 1.6 nm) to adsorbed TCNQ molecules and creates indefinitely stable ion pairs that are characterized by steady-state visible and mid-infrared absorption spectroscopy of reduced TCNQ and by NMR spectroscopy of the protons of oleate ligands that coat the QDs. The combination of these techniques shows that (i) each QD reduces an average of 4.5 TCNQ molecules, (ii) every electron transfer event between the QD and TCNQ occurs at the QD surface, (iii) sulfur ions on the surfaces of the QDs (and not delocalized states within the QDs) are the electron donors, and (iv) some TCNQ molecules adsorb directly to the surface of the QDs while others adsorb upon displacement of oleate ligands.

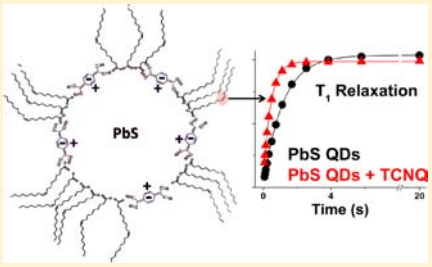


## INTRODUCTION

This paper describes the formation of a multielectron ground-state charge-transfer (CT) complex of oleate-coated PbS quantum dots (QDs) and tetracyanoquinodimethane (TCNQ) molecules. Thermodynamically spontaneous electron transfer occurs from sulfur ions on the surfaces of the QDs (radius =1.6 nm) to adsorbed TCNQ molecules, in $CHCl_3$ dispersions. The QD/TCNQ complex is a multiplexed form of a molecular CT complex, where the QD acts as a scaffold for multiple sulfur−TCNQ interactions. We use functional groups on both the electron donor (the QD) and electron acceptor (TCNQ) as probes for two of the most common and powerful structural characterization techniques, nuclear magnetic resonance (NMR) and Fourier transform infrared spectroscopy (FTIR). Using these techniques, we investigate how the chemical and electronic interaction between PbS QDs and TCNQ molecules leads to multielectron transfer and how the number of CT complexes per QD depends on the surface chemistry of the QD. Our conclusions with respect to the chemistry that promotes charge transfer are applicable to a range of spontaneous and nonspontaneous QD−ligand redox systems.

Both the cores and surfaces of QDs are potential multielectron redox centers in either the ground state or a photoexcited state of the QD, given molecular partners with the right redox potentials and adsorption characteristics. There are five previously reported mechanisms for multi-charge-transfer interactions between QDs and organic molecules: (i) Multiphoton photoexcitation into states delocalized within the core of the QD, followed by multiexciton dissociation, produces up to ∼20 coexistent charge-separated states on the surface of a QD.[1−3] (ii) Single-photon photoexcitation into a state delocalized within the core of the nanoparticle and carrier multiplication,[4,5] followed by multiexciton dissociation, can lead to external quantum efficiencies of greater than 100% in solar cells based on these materials. (iii) Ground-state CT complexes of $TiO_2$ QDs with enediols and aromatic thiols,[6,7] and of cadmium and lead chalcogenide QDs with dithiocarbamates,[8−10] have been used to investigate fundamental properties of charge carriers in the core of the QDs[9] and to study the structure of the adsorbed molecule through resonance-enhanced spontaneous Raman scattering.[6,7] (iv) Steady-state illumination of $TiO_2$ and ZnO nanoparticles, followed by sequential scavenging of photogenerated holes by solution-phase reductants or codeposited metal islands, produces up to tens of electrons that can live indefinitely in delocalized conduction band or surface-trapped states of the particle.[11−16] These "photocharged" particles can then be used as reagents for multielectron reduction of $O_2$ and $H_2O_2$ to water, reduction of nitrate ions to ammonia,[11] and proton-coupled electron transfer to phenoxyl and nitroxyl radicals.[12,13] (v) Perhaps most relevant to this work, the photoluminescence quantum yield of $Mn^{2+}$-doped ZnSe QDs increased by a factor of 5 due to spontaneous electron donation from a variety of noncoordinating molecular reductants to surface-localized midgap states of the QD. The authors in this case concluded that approximately 100 reduction events occur per QD.[17]

The challenge in optimizing each of these types of potentially very useful systems for a given application is understanding the dependence of the relevant properties of the charge-transfer process—including the lifetime of the charge-separated state,

Received: January 10, 2013
Published: April 23, 2013

   dx.doi.org/10.1021/ja4003074 | J. Am. Chem. Soc. 2013, 135, 7264−7271

number of charge-separated states that can form per particle, and degree of localization of the charge carriers within the particle—on the chemical structure of the inorganic/organic interface. Investigation of structure–function relationships in these systems is facilitated by the ability to study the charge-separated state directly, rather than inferring information about the CT process from measurements on the ground state. The lifetimes of photogenerated radical ion pairs, however, are typically on the picosecond to nanosecond timescale[2,18] and therefore can be probed only by time-resolved optical measurements. These measurements yield the rate of formation and decay of the charge-separated state but little information about the geometry or chemistry of the donor–acceptor pair. Ultrafast coherent spectroscopies can track the structure of a donor–acceptor system through the charge-separation process,[19] but the application of these techniques to charge transfer in colloidal QD systems is still too complicated (in both setup and interpretation) to be used routinely.

Here, we describe a PbS QD/TCNQ system within which the indefinite stability of the charge-separated state allows us to detect and quantify the electron transfer events through steady-state signals originating from both TCNQ and the QD, namely, visible and mid-infrared absorptions of reduced TCNQ and $^1$H NMR signals from the oleate ligands that coat the QDs. Through the combination of these techniques, we conclude that (i) each QD reduces an average of 4.5 TCNQ molecules, (ii) every electron transfer event between the QD and TCNQ occurs at the QD surface, (iii) sulfur ions on the surfaces of the QDs (and not delocalized states within the QDs) are the electron donors, and (iv) TCNQ molecules adsorb to the QD surface both directly and by displacing weakly bound lead–oleate complexes from the surface of the QD.

## RESULTS AND DISCUSSION

**Synthesis and Composition of Oleate-Coated PbS QDs, and Preparation of QD/TCNQ Mixtures.** We synthesized PbS QDs with radius 1.6 nm, as inferred from the energy of the first excitonic absorption peak at 920 nm and the calibration curve of Cademartiri et al.[20] The Supporting Information contains details of the synthesis and a histogram of radius measurements obtained from TEM images (Figure S1). The TEM measurements yield a radius of 1.8 ± 0.2 nm; however, in our estimates of surface area and chemical composition of the QD, we will use the radius obtained from the absorption spectrum because there is less error in determining the absorption wavelength than in analyzing a TEM image, and because Cademartiri's calibration curve is based on measurements of many sizes of QDs.

Figure 1A is a cartoon of our estimated composition of the QDs. We see no evidence of protonated oleic acid, which serves as surfactant in the reaction mixture, in the form of O–H or carbonyl stretches in the FTIR spectrum of these QDs after purification; we observe only features corresponding to deprotonated carboxylates (see Figure S4 in Supporting Information). This result indicates that, in the final ligand shell of the QDs, the oleic acid binds only as oleate to $Pb^{2+}$. The presence of anionic surfactant in the reaction mixture drives $Pb^{2+}$ enrichment of the surfaces of the QDs, as we have observed previously for CdSe.[21] We measure, through inductively coupled plasma atomic emission spectroscopy (ICP-AES), a molar ratio Pb:S of 1.61:1. This ratio, given the surface area of the particles and the ionic radius of $Pb^{2+}$, translates into ~30% of a complete monolayer of $Pb^{2+}$ on the surfaces of the QDs, where the excess $Pb^{2+}$ is adsorbed on surface sulfur as lead oleate. NMR measurements indicate that there are ~150 oleate ligands/QD (~4.8 oleate ligands/nm$^2$). The Supporting Information contains details of the ICP-AES and FTIR measurements and analysis, and the calculation of surface composition.

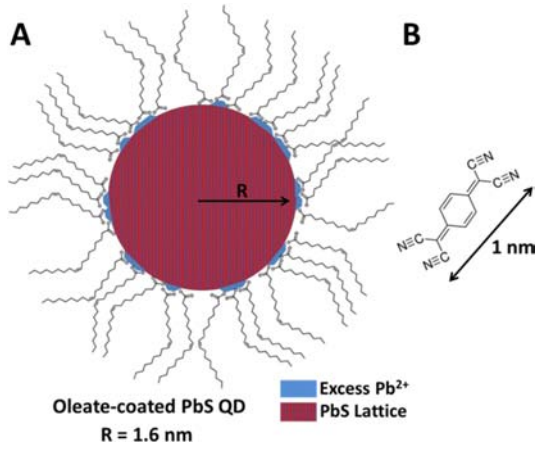


**Figure 1.** (A) Cartoon of oleate-coated PbS QDs showing submonolayer coverage of the stoichiometric PbS surface with excess $Pb^{2+}$. NMR measurements indicate that there are approximately 150 oleate ligands/PbS QD (~4.8 oleate ligands/nm$^2$); see Supporting Information. (B) Structure of the electron acceptor tetracyanoquinodimethane (TCNQ).

We purchased TCNQ (Figure 1B) from Sigma–Aldrich and used it as received.

All PbS QD-TCNQ mixtures equilibrated in either $CHCl_3$ or $CDCl_3$ for at least 1 h before NMR or absorption spectra were acquired; see Supporting Information for details of sample preparation for each measurement. No care was taken to avoid exposure of the samples to room light during preparation or measurement. A separate experiment carried out in the dark confirms that the production of reduced TCNQ in the presence of QDs is completely insensitive to the flux of photons through the sample, and thus, the charge-transfer process is spontaneous (see Figure S3 in Supporting Information).

**Electron Transfer Occurs Spontaneously from PbS QDs to TCNQ.** We used features in the visible and mid-IR absorption spectra of TCNQ and in NMR spectra of oleate ligands on the surface of the QDs to confirm that charge transfer occurs between the PbS QDs and TCNQ and to characterize the QD/TCNQ charge-transfer complex.

*Visible and Mid-IR Absorption Spectra of QD/TCNQ Mixtures Have Features Corresponding to Reduced TCNQ.* Figure 2A shows three spectra: (i) the absorption spectrum of $1.6 \times 10^{-5}$ M PbS QDs in $CHCl_3$ with no added TCNQ (black), (ii) the absorption spectrum of the same concentration of QDs mixed with a 13-fold excess of TCNQ in $CHCl_3$ (red), and (iii) the spectrum of TCNQ that has been reduced to its radical anion, $TCNQ^{\bullet -}$, electrochemically in $CH_2Cl_2$ (blue). The peaks at 686, 749, and 850 nm (and associated side bands) in spectra iii (blue) and ii (red) correspond to characteristic absorptions of partially or fully reduced TCNQ; these features also appear in metal and organic charge-transfer complexes of TCNQ,[22−25] and their energies appear to be insensitive to the type of charge-transfer complex and the solvent (compare, for example,[22,24,25] see Supporting Information).


dx.doi.org/10.1021/ja4003074 | J. Am. Chem. Soc. 2013, 135, 7264−7271

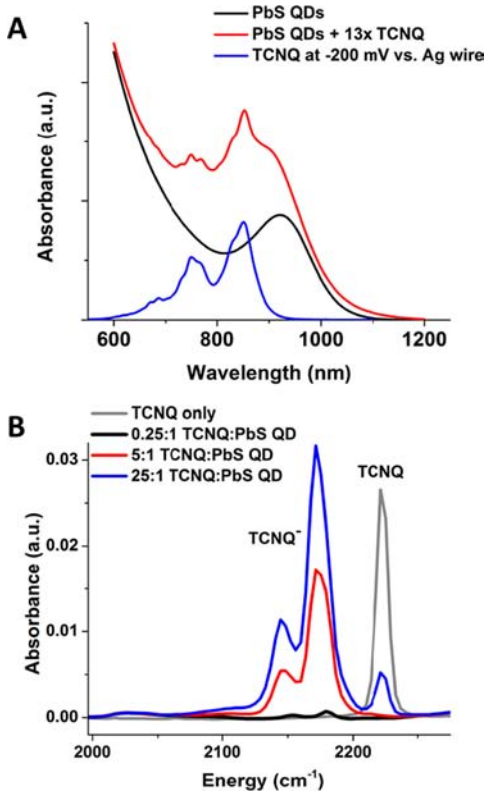


**Figure 2.** (A) Absorption spectrum of $1.6 \times 10^{-5}$ M PbS QDs in $CHCl_3$ with no added TCNQ (black), the spectrum of the same concentration of QDs mixed with a 13-fold excess of TCNQ in $CHCl_3$ (red), and for comparison, the spectrum of 0.018 M TCNQ (no QDs) that has been reduced to its radical anion electrochemically by applying a constant potential of −200 mV vs an Ag wire pseudoreference (0.1 M TBAP, Pt wire counter electrode, Pt mesh working electrode) in $CH_2Cl_2$ (blue). All spectra were measured in ambient atmosphere. (B) C−N stretching region of the FTIR spectra of a series of PbS−TCNQ mixtures with selected TCNQ:PbS ratios indicated in the legend. The peak at 2222 $cm^{-1}$ corresponds to neutral TCNQ; it disappears when PbS QDs are in molar excess of TCNQ, but reappears upon adding 5× excess TCNQ to QDs. The pairs of peaks at 2179/2154 $cm^{-1}$ (black trace), and 2173/2145 $cm^{-1}$ (blue and red traces) correspond to reduced TCNQ, which is always present in mixtures of TCNQ with PbS QDs. The concentration of the TCNQ-only sample is $1 \times 10^{-3}$ M. The concentration of QDs in this set of samples is constant at $1 \times 10^{-4}$ M.

The overlap of the reduced TCNQ spectrum in the visible region with the ground-state spectrum of the PbS QDs complicates quantitative analysis of the spectra in this region. We therefore also monitored the electronic state of TCNQ within a series of PbS QD/TCNQ mixtures in the nitrile stretching region of the mid-IR, 2100−2300 $cm^{-1}$. Figure 2B shows spectra at select molar ratios of TCNQ:QD in $CHCl_3$; see Figure S5 in Supporting Information for spectra at additional molar ratios and spectra acquired in $CDCl_3$ for direct comparison with NMR data. Within this region, the single peak at 2222 $cm^{-1}$ corresponds to neutral TCNQ, and the pair of peaks in the 2145−2180 $cm^{-1}$ region indicates the presence of TCNQ with anionic character. We always observe peaks corresponding to reduced TCNQ in mixtures of TCNQ with PbS QDs. In samples where TCNQ:PbS ≤ 5:1, we observe only features corresponding to reduced TCNQ; in samples where TCNQ:PbS > 5:1, the neutral TCNQ species is also detectable. The progression of these IR spectra indicates that the production of reduced TCNQ occurs with 100% yield until it is at a 5:1 excess; at >5:1 excess, reduced TCNQ is formed with less than 100% yield until its production saturates at TCNQ:PbS ∼ 25:1. Importantly, the IR measurement, unlike NMR, distinguishes between TCNQ molecules different adsorption or oxidation states, even if those states are in fast exchange with each other. The peaks in the IR spectrum may therefore be broadened by heterogeneity in the oxidation state of TCNQ molecules in the sample at any given time, but the peak positions are not time-averages of the states of TCNQ molecules.

*NMR Spectra of QD/TCNQ Mixtures Indicate the Presence of Paramagnetic Centers at the Surfaces of QDs.* Figure 3A shows the NMR spectra of a $CDCl_3$ solution of free TCNQ

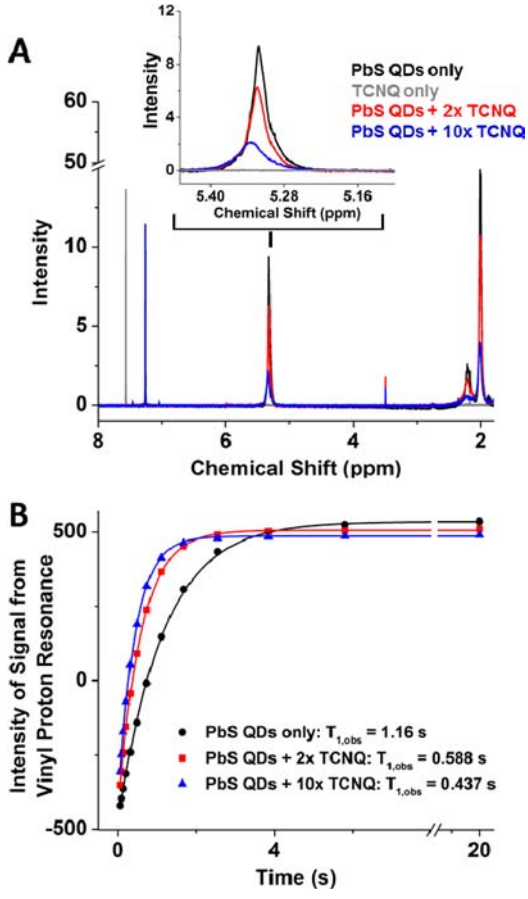


**Figure 3.** (A) $^1H$ NMR spectra of free TCNQ (gray) and TCNQ/PbS QD mixtures with 0 (black), 2 (red), and 10 (blue) TCNQ molecules added per QD, in $CDCl_3$. The spectrum of the TCNQ-only sample has a singlet peak at 7.55 ppm. This signal disappears in the presence of any amount of added QDs (molar ratios of TCNQ:QD ranging from 0.005:1 to 20:1). The peaks at 2.0, 2.2, and 5.3 ppm correspond to the protons of oleate ligands on the surfaces of the QDs. The signal at 3.5 ppm corresponds to residual methanol used in the purification of the QDs. (Inset) Zoom-in of the vinyl region of oleate spectra for these samples. The peak shifts to higher ppm and broadens upon addition of TCNQ. (B) Kinetics of spin−lattice-mediated ($T_1$) decay of signal at 5.3 ppm (vinyl protons of oleate) in the same set of PbS QD/TCNQ samples as shown in panel A. The kinetic traces fit to single-exponential functions with time constants $T_{1,obs}$. The value of $T_{1,obs}$ decreases with increasing amounts of added TCNQ. The Supporting Information contains NMR spectra and $T_1$ kinetics for additional molar ratios of TCNQ:QD and for other proton resonances within these spectra. The peak at 7.26 ppm corresponds to $CHCl_3$.


dx.doi.org/10.1021/ja4003074 | J. Am. Chem. Soc. 2013, 135, 7264−7271

(no added QDs, gray), and of TCNQ/PbS QD mixtures with 0 (black), 2 (red), and 10 (blue) TCNQ molecules added per QD (see Figure S6A in Supporting Information for spectra of mixtures with additional molar ratios between 0.01 and 20 TCNQ:QD). The spectrum of the TCNQ-only sample has a singlet peak at 7.55 ppm. In all the mixtures of TCNQ and QDs, we monitored the spectra over a range of −150 to 350 ppm, and did not observe any peak corresponding to the TCNQ protons. We interpret the complete disappearance of this signal, even in mixtures with large excess of TCNQ, as an indication that, within the NMR time scale (∼1 s), every TCNQ in the sample is near a paramagnetic center (or is paramagnetic itself).[26]

Clearly, we cannot use the NMR signal from TCNQ to monitor the charge-transfer process, so we instead use signals from the QDs, specifically signals from the protons of the oleate ligands on the QDs. The peaks at 2.0, 2.2, and 5.3 ppm (and alkyl peaks below 2 ppm, not shown) correspond to the protons of these oleate ligands. Even in the absence of TCNQ, these resonances are broadened relative to those of freely diffusing oleate because they are adsorbed to a slow-tumbling particle.[27] The inset of Figure 3A focuses on the resonance of the vinyl protons of oleate. This peak shifts to higher ppm and broadens further upon addition of TCNQ; this behavior is representative of all the oleate protons in the sample. The integrated area of this peak does not change (indicating no degradation of oleate) with added TCNQ; see Figure 6B in Supporting Information.

Figure 3B shows kinetic traces of $T_1$ decay of the signal at 5.3 ppm (vinyl protons of oleate) in the same set of PbS QD/TCNQ samples as shown in Figure 3A. Each kinetic trace fits to a single-exponential function with time constant $T_{1,obs}$, which decreases with increasing amounts of added TCNQ. Figure S7 in Supporting Information contains $T_1$ kinetic traces for other oleate proton resonances. One interpretation of this acceleration of the $T_1$ relaxation process for oleate protons is that, with increasing amounts of TCNQ present, an increasing fraction of oleate protons on the surfaces of the QDs are near a paramagnetic center.[28] From the value of $T_{1,obs}$ for a proton within a given QD/TCNQ mixture, the paramagnetic contribution to relaxation, $T_{1P}$, is given by

$$\frac{1}{T_{1,obs}} = \frac{1}{T_1} + \frac{1}{T_{1P}} \quad (1)$$

where $T_1$ is the intrinsic relaxation time of the proton with no paramagnetic centers present.[28]

*Correlation of NMR and IR Data Indicates That Paramagnetism in QD/TCNQ Mixtures Is Due to Electron Transfer.* Figure 4A shows a plot (red symbols, left axis) of $1/T_{1P}$, obtained from eq 1, for the vinyl protons (5.3 ppm) of oleate on the surfaces of PbS QDs versus the molar ratio TCNQ:PbS in mixtures of TCNQ and QDs in $CDCl_3$. This plot is representative of that for other oleate protons (see Supporting Information). The same graph (black symbols, right axis) includes FTIR data: a plot of the intensity of the larger of the two peaks corresponding to the C−N stretching mode (2173−2179 $cm^{-1}$) of reduced TCNQ versus the molar ratio TCNQ:PbS in mixtures of TCNQ and PbS QDs in $CDCl_3$ (■) and $CHCl_3$ (□). We gathered the NMR and FTIR data from six separately prepared sets of PbS QD/TCNQ mixtures.

The identical dependence of spin−lattice relaxation rate of oleate vinyl protons and the concentration of TCNQ anion in

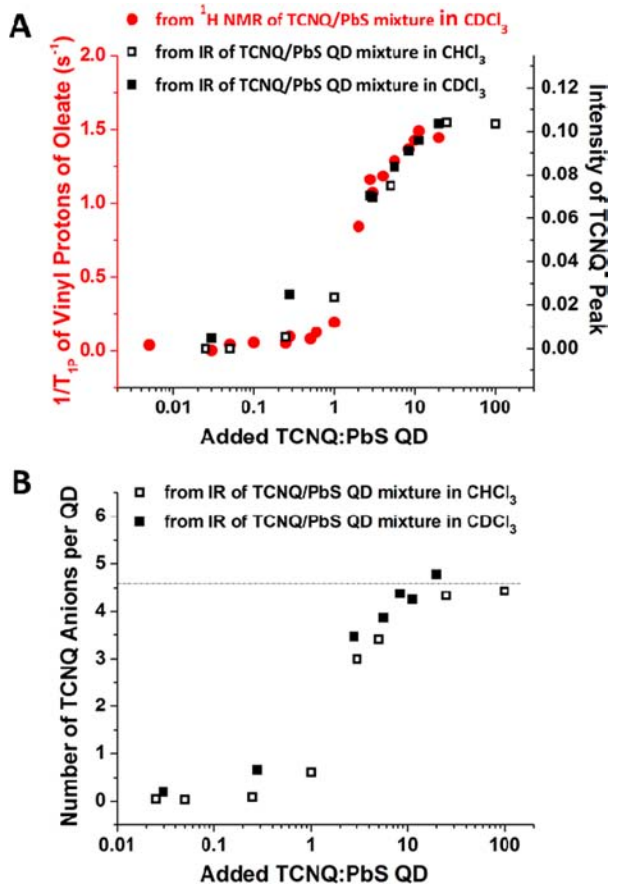


**Figure 4.** (A) (Left axis, red) Plot of $1/T_{1P}$, obtained from eq 1, for vinyl protons (5.3 ppm) of oleate on the surfaces of PbS QDs vs molar ratio TCNQ:QD in mixtures of TCNQ and PbS QDs in $CDCl_3$. (Right axis, black) Plot of intensity of the peak corresponding to the C−N stretching mode of reduced TCNQ vs molar ratio TCNQ:PbS in mixtures of TCNQ and PbS QDs in $CDCl_3$ (■) and $CHCl_3$ (□). The overlap of NMR and IR data sets indicates that electron transfer to TCNQ is responsible for creation of paramagnetic centers at the surface of the QD. (B) Plot of number of reduced TCNQ molecules per QD vs molar ratio TCNQ:QD in mixtures of TCNQ and PbS QDs in $CDCl_3$ (■) and $CHCl_3$ (□). The Supporting Information details our procedure for determining the number of reduced TCNQ molecules in a sample.

solution on the molar ratio TCNQ:QD, apparent in the overlap of black and red symbols in Figure 4A, shows that the acceleration of $T_1$ relaxation of oleate protons is precisely correlated with creation of paramagnetic centers by electron transfer from QDs to TCNQ[29] and strongly suggests that the source of perturbation to $T_1$ is the paramagnetic centers formed upon electron transfer. In order to rule out the possibility that the change in $T_1$ is due to a TCNQ-induced change in the binding equilibrium of oleate with the QDs, and therefore a change in their average tumbling time, we measured the average diffusion constant of oleate within a series of mixtures of the PbS QDs and TCNQ by diffusion-ordered NMR spectroscopy (DOSY NMR). This experiment, which is explained in detail in the Supporting Information, shows that, at sufficiently high concentrations of TCNQ, TCNQ does displace oleate. The dependence of the average diffusion constant of oleate on the molar ratio TCNQ:QD does not, however, match the dependence of $T_1$ on the molar ratio TCNQ:QD (see Supporting Information). Furthermore, for the set of hydro-


dx.doi.org/10.1021/ja4003074 | J. Am. Chem. Soc. 2013, 135, 7264−7271

dynamic radii relevant for displaced oleate and oleate on the QD, we would expect $T_1$ to *increase* (i.e., the proton resonance to sharpen) upon displacement by TCNQ,[30] when in fact, we observe that $T_1$ decreases (and the signal broadens) during titration of the QDs with TCNQ. The DOSY data are evidence that a change in binding equilibrium of oleate with the QD upon addition of TCNQ is not responsible for the change in $T_1$ that we observe, and they further support our assertion that $T_1$ changes due to creation of paramagnetic centers by electron transfer. The overlap of NMR and IR data in Figure 4A also shows that no TCNQ anion is created without perturbation of the $T_1$ relaxation time of surface-bound oleate,[31] so electron transfer must occur on the surface of the QD.

By calculating the absorption coefficient for the nitrile stretching mode in $CHCl_3$ and $CDCl_3$ (see Supporting Information), we determined that, at the molar ratio at which formation of TCNQ anion saturates (~20:1 TCNQ:QD), an average of 4.5 TCNQ anions are present per QD in the mixture (Figure 4B).

**TCNQ Oxidizes Sulfur on the Surface of QDs.** Quantum dots have both localized and delocalized orbitals within their nanocrystalline cores, on their inorganic surfaces, and within their ligand shells, and any of these orbitals could in principle be responsible for reducing TCNQ. The ionization potential of the delocalized valence band of 1.6-nm PbS QDs (which is 75% sulfur 3p orbitals)[32] is measured to be −5.0 versus vacuum (+0.21 V versus standard calomel electrode, SCE), based on UV photoemission spectroscopy.[33] It is therefore possible—given the error in using a potential measured in the solid state to predict a potential in solution—that the QD core could serve as an electron donor to TCNQ, which has a reduction potential of +0.13 V versus SCE in acetonitrile (−4.9 versus vacuum; see Supporting Information), to create a delocalized hole. In the region of the IR spectrum where previous work has detected intraband transitions of delocalized holes in the valence band of PbS QDs (which peak at ~2000 $cm^{-1}$),[34] we see no evidence of this intraband transition: the spectrum of PbS QDs without added TCNQ matches that with TCNQ (at 25:1 TCNQ:QD) over a range of 2000 $cm^{-1}$, aside from features due to TCNQ itself and small perturbations to the oleate signals,[35] probably due to TCNQ adsorption (see Figure S12 in Supporting Information). The other sign of the presence of a delocalized hole in the QD valence band is bleaching of the first excitonic feature of the ground-state absorption.[36−38] A five-electron oxidation of a PbS QD core should produce more than a 50% bleach of its ground-state absorption.[39,40] We do not observe such a bleach in Figure 2A. Both the visible and IR absorption spectra of PbS QD/TCNQ complexes therefore suggest that the electron donor is a localized state on the surface of the QD, not a delocalized state of the core.

Neither $Pb^{2+}$ ions nor oleate appears to be the electron donor: integration of the peak corresponding to the vinyl protons of oleate in the NMR does not change with added TCNQ, and a mixture of Pb−$(oleate)_2$ (a molecular source of oleate and $Pb^{2+}$) and TCNQ in the absence of QDs produces no reduced TCNQ. A mixture of TCNQ with TMS sulfide (a molecular source of $S^{2-}$), however, does contain reduced TCNQ; see Figure S12 in Supporting Information. These results strongly suggest that sulfur is the electron donor to TCNQ. NMR spectroscopy confirms that the PbS QD sample is purified of all of the molecular starting materials for the QD reaction—TMS sulfide, Pb−$(oleate)_2$, and octadecene (see Supporting Information)—so it is sulfur on the surface of the QD that is responsible for reduction of TCNQ. X-ray photoelectron spectroscopy indicates that the oxidation state of sulfur is 2− within the PbS lattice of the QD core, and primarily 2− and 1− on the surface of the QD. The surface does contain sulfur in a range of oxidation states from 2− to 2+, however (see Figure S13 in Supporting Information).

The assignment of surface sulfur ions as the electron donors to TCNQ is not surprising. Bard and co-workers[41] found that the electrochemical oxidation of PbS QDs (4.2 nm diameter, deposited on a gold electrode with aqueous electrolyte), proceeds through two-electron oxidation of $S^{2-}$ at +0.25 V versus SCE, independent of particle size. The first oxidation probably occurs closer to the potential at the onset of current (~+0.1 V versus SCE). Another group reported a potential of +0.144 V versus SCE (with aqueous electrolyte) for two-electron oxidative dissolution of a film of PbS to form elemental sulfur.[42] Oxidation of $S^{2-}$ does not have to proceed to elemental sulfur: Au(I) complexes with dithiolates with extended ring systems undergo one-electron dithiolate-centered oxidation in the presence of TCNQ, confirmed by the presence of TCNQ anion in the IR spectrum.[43] If it is assumed that one-electron oxidation of sulfur on the surface of the QDs occurs between +0.1 V and +0.2 V versus SCE, then the highest occupied molecular orbital (HOMO) of these localized sulfur ions has an energy that is just within the bandgap of the QD.

We do not know from our experiments whether the paramagnetism that perturbs spin−lattice relaxation of the oleate molecules comes solely from reduced TCNQ or if the surface of the QD is also paramagnetic after charge transfer. Paramagnetic organosulfur species have been produced by irradiating the sulfur species with UV light, as evidenced by electron paramagnetic resonance (EPR) spectra,[44] but we do not know whether sulfur radicals are stable on the surface of PbS QDs; this topic will be the subject of future study.

**TCNQ Adsorbs to the QD in Two Geometries.** Inspection of the IR spectra of QD/TCNQ mixtures in the nitrile region of TCNQ (Figure 2B and Figure S5 in Supporting Information) reveals that, at molar ratios TCNQ:QD ≤ 1:1, the two C−N stretching peaks corresponding to reduced TCNQ have maxima at 2179 and 2154 $cm^{-1}$, respectively. At TCNQ:QD > 1:1, these two peaks shift to lower energy to 2173 and 2145 $cm^{-1}$, respectively. The transition between these two regimes is sharp; it occurs completely between 1:1 and 3:1 TCNQ:QD, as if the system were accessing a second state (Figure 5, red solid circles, left axis). When the peaks of these anion features shift to 2173 and 2145 $cm^{-1}$, they also broaden to include the peaks at 2179 and 2154 $cm^{-1}$; the system therefore does not transition entirely to this second state but rather evolves to include TCNQ molecules in both states. It is well-documented that the energy of the C−N stretching features shift to lower energy as more electron density is deposited in the C−N antibonding orbital.[25,29,45−48] We can conclude from Figure 5 that, between TCNQ:QD = 1 and 3, TCNQ begins to adsorb to the QD in a new geometry that leads to a different electron distribution in its lowest unoccupied molecular orbital (LUMO). Comparison of the energy of either of the C−N stretching peaks (we chose the higher-energy one) with the average diffusion coefficient of oleate in the system, as obtained with DOSY NMR (Figure 5, black solid circles, right axis) shows that at the same point in the titration that the TCNQ begins to adsorb in this new geometry (~3:1 TCNQ:QD), the average diffusion constant of oleate in the system increases (see Figure S9 in the Supporting


dx.doi.org/10.1021/ja4003074 | J. Am. Chem. Soc. 2013, 135, 7264−7271

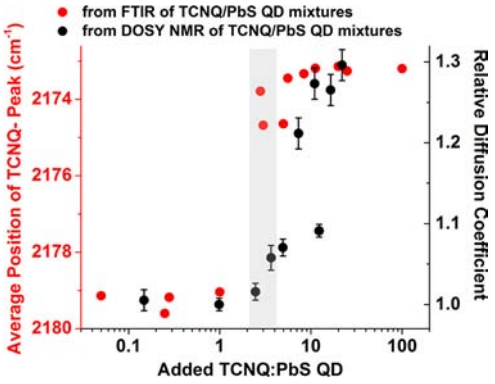


**Figure 5.** (Left axis, red) Plot of average frequency of the dominant C−N stretching peak ($cm^{-1}$) for reduced TCNQ, weighted by respective contributions of the ∼2179 and 2173 $cm^{-1}$ components, vs molar ratio TCNQ:PbS in mixtures of TCNQ and PbS QDs in $CHCl_3$ (red symbols). (Right axis, black) Average diffusion coefficient of oleate in the TCNQ/PbS QD mixtures, relative to the diffusion coefficient in the absence of TCNQ. An increase in the relative diffusion coefficient corresponds to displacement of oleate from the surface of the QD. The error bars represent error in the fit of the DOSY data (see Supporting Information). The gray box highlights the molar ratio TCNQ:QD at which we observe both an onset of this displacement and an effective shift of the FTIR spectrum of reduced TCNQ.

Information). The DOSY NMR time scale is ∼100 ms, so the diffusion constant for oleate molecules in fast exchange between free and bound states is a weighted average of the diffusion constants in the two states. An increase in the average diffusion constant indicates that TCNQ is displacing some oleate molecules from the surfaces of the QDs. The shift in peak energy in the IR, and the appearance of the new adsorption geometry to which it corresponds, is therefore correlated with this displacement.

Our previous studies of photoinduced electron transfer processes involving PbS QDs have shown that QDs of this size have 1−2 "empty" sites, that is, sites on the QD where a small molecule can adsorb directly without displacing ligands or surface ions (probably due to a gap in the ligand shell).[49] We therefore suspect that the dominant adsorption geometry at low TCNQ:QD ratios (the geometry that results in IR features at 2179 and 2154 $cm^{-1}$) corresponds to adsorption at these empty sites. Once these sites fill, TCNQ must displace ligands in order to adsorb, and this leads to an adsorption geometry that results in IR features at 2173 and 2145 $cm^{-1}$, which become more prominent as TCNQ:QD increases. Oleate presumably dissociates from the surface of the QD as the neutral complex Pb−$(oleate)_2$ or a neutral lead−oleate cluster; dissociation without accompanying $Pb^{2+}$ requires protonation by a free oleic acid molecule,[50] and we see no evidence of protonated oleic acid in the IR spectra of these QDs.

The total number of TCNQ molecules that each QD can reduce is therefore limited by the number of "empty sites" plus the number of loosely bound lead oleate groups on the surface of the QD, which is a function of the size and surface structure of the QD.[51] For these particular QDs, the total number of sites that are either empty or accessible through displacement of weakly bound lead oleate is approximately 5. Future work will explore the dependence of this number on the size and surface structure of the QD.

## CONCLUSION

We have demonstrated that PbS QDs with radii of 1.6 nm, coated in oleate ligands, form multielectron charge-transfer complexes with TCNQ acceptors. Addition of TCNQ to PbS QDs in $CHCl_3$ (or $CDCl_3$) results in spontaneous formation of features in the visible and mid-IR (Figure 2) absorption spectra of the mixture that correspond to reduced TCNQ. The spin−lattice relaxation time of oleate protons and the concentration of reduced TCNQ have identical dependencies on the molar ratio TCNQ:QD (Figure 4A), so we conclude that the decrease in $T_{1,obs}$ we observe is due to the formation of paramagnetic centers upon electron transfer from the QD to TCNQ, and that every electron transfer event occurs at the QD surface. We observe no features corresponding to delocalized holes that would form upon oxidation of the QD core in the near- or mid-IR absorption spectra of the QDs. The absence of these features, in conjunction with evidence that a molecular source of $S^{2-}$ reduces TCNQ (but a molecular source of $Pb^{2+}$ does not), allows us to conclude that sulfur anions on the surfaces of the QDs are the electron donors to TCNQ. The maximum number of reduced TCNQ molecules formed per QD is 4.5 (Figure 4B). The number of TCNQ molecules a QD is able to reduce likely depends on the number of available adsorption sites for TCNQ on the QD surface, present either initially or made available by displacement of weakly bound $Pb^{2+}$−oleate complexes from the surface of the QD.

There are two major consequences of thermodynamic spontaneity of the electron-transfer reaction between PbS QDs and TCNQ: (i) We can obtain mechanistic information about the electron-transfer process with a wide variety of steady-state chemical and optical characterization methods, whereas the short-lived charge-separated states created by photoinduced electron transfer are usually observable only through time-resolved optical methods. Monitoring the response of spin−lattice relaxation times of oleate ligands on the QD to charge separation allows us to confirm that electron transfer is occurring on the surface of the QD and to elucidate the role of surface ligand displacement in the formation of donor−acceptor complexes. This type of information will also be useful in analyzing and optimizing systems for photoinduced multi-electron-transfer processes involving QDs. (ii) The indefinitely stable charge-separated state can potentially be used to catalyze processes, like redox-triggered chemical reactions, that are not fast enough to use electrons with recombination-limited lifetimes of microseconds or less.

Point ii raises an issue with the utility of this specific system: electron transfer from the ground state of the QD to TCNQ is possible because TCNQ is somewhat of an electron "sink": its reduction potential is ∼800 mV below that of a proton. The more interesting application of this ground-state charge-transfer interaction is as a means to postsynthetically "dope" QDs within a film, with four potential benefits for charge transport through a QD-based material:[52] (i) Excess electron density in the surrounding ligand shell of the QD (due to charge transfer to TCNQ ligands) reduces the potential barrier for holes to tunnel between QDs within the film and homogenizes the energy landscape for their transport. (ii) TCNQ fills hole traps on the surfaces of the QDs by oxidizing undercoordinated sulfur ions, thus increasing the lifetime of mobile holes within the material. (iii) Formation of anionic TCNQ introduces new absorption bands in a region of minimum absorption by the QD (700−900 nm), a region of high spectral irradiance.[53]


dx.doi.org/10.1021/ja4003074 | J. Am. Chem. Soc. 2013, 135, 7264−7271

These absorptions excite electrons to LUMO + $x$ states of prereduced TCNQ; electrons in these states have similar energy to those in the excited states of the QDs formed by photoexcitation in this region (since the LUMO of TCNQ is approximately degenerate with the HOMO of the QD). Even though the mixing between the LUMO of TCNQ and the HOMO of the QD is not strong enough to perturb the absorption spectrum of the TCNQ anion, these electrons will contribute to the concentration of mobile carriers. (iv) Within composite films of QDs and conjugated polymer, adsorbed TCNQ molecules have been shown to facilitate electronic interaction between the QD and the polymer by enhancing the dispersibility of the QDs within the polymer.[54] All four of these effects are potentially beneficial to the photovoltaic efficiency of QD/TCNQ-based active materials.

## ■ ASSOCIATED CONTENT

### Supporting Information

Additional text, 13 figures, and two tables with details of synthesis, measurements, and sample prep; TEM images of QDs; cyclic voltammetry of TCNQ; additional FTIR and NMR spectra; $T_1$ relaxation kinetics; calculation of number of reduced TCNQ per QD and QD surface composition; and XPS and DOSY NMR spectra. This material is available free of charge via the Internet at http://pubs.acs.org.

## ■ AUTHOR INFORMATION

### Corresponding Author

e-weiss@northwestern.edu

### Notes

The authors declare no competing financial interest.

## ■ ACKNOWLEDGMENTS

This work was supported by a grant from the Air Force Office of Scientific Research (AFOSR) (FA9550-10-1-0220) through a Young Investigator Award to E.A.W. K.E.K. is supported by the Department of Energy Office of Science Graduate Fellowship Program (DOE SCGF), made possible in part by the American Recovery and Reinvestment Act of 2009, administered by ORISE-ORAU under Contract DE-AC05-06OR23100.

## ■ REFERENCES

(1) Zhu, H.; Song, N.; Rodriguez-Cordoba, W.; Lian, T. *J. Am. Chem. Soc.* **2012**, *134*, 4250.
(2) Huang, J.; Huang, Z.; Yang, Y.; Zhu, H.; Lian, T. *J. Am. Chem. Soc.* **2010**, *132*, 4858.
(3) Zhu, H.; Lian, T. *J. Am. Chem. Soc.* **2012**, *134*, 11289.
(4) Sambur, J. B.; Novet, T.; Parkinson, B. A. *Science* **2010**, *330*, 63.
(5) Semonin, O. E.; Luther, J. M.; Choi, S.; Chen, H.-Y.; Gao, J.; Nozik, A. J.; Beard, M. C. *Science* **2011**, *334*, 1530.
(6) Musumeci, A.; Gosztola, D.; Schiller, T.; Dimitrijevic, N. M.; Mujica, V.; Martin, D.; Rajh, T. *J. Am. Chem. Soc.* **2009**, *131*, 6040.
(7) Fu, X.; Pan, Y.; Wang, X.; Lombardi, J. R. *J. Chem. Phys.* **2011**, *134*, No. 024707.
(8) Frederick, M. T.; Weiss, E. A. *ACS Nano* **2010**, *4*, 3195.
(9) Frederick, M. T.; Cass, L. C.; Amin, V. A.; Weiss, E. A. *Nano Lett.* **2011**, *11*, 5455.
(10) Frederick, M. T.; Amin, V. A.; Swenson, N. K.; Ho, A. Y.; Weiss, E. A. *Nano Lett.* **2013**, *13*, 287.
(11) Mohamed, H. H.; Mendive, C. B.; Dillert, R.; Bahnemann, D. W. *J. Phys. Chem. A* **2011**, *115*, 2139.
(12) Schrauben, J. N.; Hayoun, R.; Valdez, C. N.; Braten, M.; Fridley, L.; Mayer, J. M. *Science* **2012**, *336*, 1298.
(13) Hayoun, R.; Whitaker, K. M.; Gamelin, D. R.; Mayer, J. M. *J. Am. Chem. Soc.* **2011**, *133*, 4228.
(14) Wood, A.; Giersig, M.; Mulvaney, P. *J. Phys. Chem. B* **2001**, *105*, 8810.
(15) Liu, W. K.; Whitaker, K. M.; Smith, A. L.; Kittilstved, K. R.; Robinson, B. H.; Gamelin, D. R. *Phys. Rev. Lett.* **2007**, *98*, No. 186804.
(16) Schimpf, A. M.; Ochsenbein, S. T.; Buonsanti, R.; Milliron, D. J.; Gamelin, D. R. *Chem. Commun. (Cambridge, U. K.)* **2012**, *48*, 9352.
(17) Rinehart, J. D.; Weaver, A. L.; Gamelin, D. R. *J. Am. Chem. Soc.* **2012**, *134*, 16175.
(18) Morris-Cohen, A. J.; Frederick, M. T.; Cass, L. C.; Weiss, E. A. *J. Am. Chem. Soc.* **2011**, *133*, 10146.
(19) Frontiera, R. R.; Fang, C.; Dasgupta, J.; Mathies, R. A. *Phys. Chem. Chem. Phys.* **2012**, *14*, 405.
(20) Cademartiri, L.; Montanari, E.; Calestani, G.; Migliori, A.; Guagliardi, A.; Ozin, G. A. *J. Am. Chem. Soc.* **2006**, *128*, 10337.
(21) Morris-Cohen, A. J.; Frederick, M. T.; Lilly, G. D.; McArthur, E. A.; Weiss, E. A. *J. Phys. Chem. Lett.* **2010**, *1*, 1078.
(22) Hartmann, H.; Sarkar, B.; Kaim, W.; Fiedler, J. *J. Organomet. Chem.* **2003**, *687*, 100.
(23) Tanner, D. B.; Miller, J. S.; Rice, M. J.; Ritsko, J. J. *Phys. Rev. B* **1980**, *21*, 5835.
(24) de Caro, D.; Jacob, K.; Souque, M.; Valade, L. www.intechopen.com, 141.
(25) de P. Silva, M. d. S.; Diogenes, I. C. N.; de F. Lopes, L. G.; de Sousa Moreira, I.; de Carvalho, I. M. M. *Polyhedron* **2009**, *28*, 661.
(26) Bakhmutov, V. I. *Practical NMR Relaxation for Chemists*; John Wiley & Sons, Ltd.: Chichester, U.K., 2004.
(27) Morris-Cohen, A. J.; Malicki, M.; Peterson, M. D.; Slavin, J. W. J.; Weiss, E. A. *Chem. Mater.* **2012**, *25*, 1155−1165.
(28) Li, Y.; Lei, X.; Lawler, R. G.; Murata, Y.; Komatsu, K.; Turro, N. J. *J. Phys. Chem. Lett.* **2010**, *1*, 2135.
(29) Ballester, L.; Barral, M. C.; Jiminez-Aparicio, R.; Olombrada, B. *Polyhedron* **1996**, *15*, 213.
(30) Bloembergen, N.; Purcell, E. M.; Pound, R. V. *Phys. Rev.* **1948**, *73*, 679.
(31) Moreels, I.; Fritzinger, B.; Martins, J. C.; Hens, Z. *J. Am. Chem. Soc.* **2008**, *130*, 15081.
(32) Kane, R. S.; Cohen, R. E.; Silbey, R. *J. Phys. Chem.* **1996**, *100*, 7928.
(33) Jasieniak, J.; Califano, M.; Watkins, S. E. *ACS Nano* **2011**, *5*, 5888.
(34) Yang, Y.; Rodriguez-Cordoba, W.; Lian, T. *J. Am. Chem. Soc.* **2011**, *133*, 9246.
(35) Wang, S.; Yue, F. J.; Wu, D.; Zhang, F. M.; Zhong, W.; Du, Y. W. *Appl. Phys. Lett.* **2009**, *94*, No. 012507.
(36) Wehrenberg, B. L.; Guyot-Sionnest, P. *J. Am. Chem. Soc.* **2003**, *125*, 7806.
(37) Wehrenberg, B. L.; Wang, C.; Guyot-Sionnest, P. *J. Phys. Chem. B* **2002**, *106*, 10634.
(38) Zhang, J.; Jiang, X. *Appl. Phys. Lett.* **2008**, *92*, No. 141108.
(39) Wang, C.; Shim, M.; Guyot-Sionnest, P. *Science* **2001**, *291*, 2390.
(40) Wehrenberg, B. L.; Yu, D.; Ma, J.; Guyot-Sionnest, P. *J. Phys. Chem. B* **2005**, *109*, 20192.
(41) Ogawa, S.; Hu, K.; Fan, F.-R. F.; Bard, A. J. *J. Phys. Chem. B* **1997**, *101*, 5707.
(42) Davis, A. P.; Huang, C. P. *Langmuir* **1991**, *7*, 803.
(43) Ryowa, T.; Nakano, M.; Tamura, H.; Matsubayashi, G.-e. *Inorg. Chim. Acta* **2004**, *357*, 3532.
(44) Tappel. *J. Chem. Phys.* **1964**, *41*, 1996.
(45) Chappell, J. S.; Bloch, A. N.; Bryden, W. A.; Maxfield, M.; Poehler, T. O.; Cowan, D. O. *J. Am. Chem. Soc.* **1981**, *103*, 2442.
(46) Zehe, A.; Robles Martinez, J. G. *J. Mol. Struct.* **2004**, *709*, 215.
(47) Butler, M. A.; Wudl, F.; Soos, Z. G. *Phys. Rev. B* **1975**, *12*, 4708.
(48) Gross-Lannert, R.; Kaim, W.; Olbrich-Deubner, B. *Inorg. Chem.* **1990**, *29*, 5046.
(49) Morris-Cohen, A. J.; Vasilenko, V.; Amin, V. A.; Reuter, M.; Weiss, E. A. *ACS Nano* **2012**, *6*, 557.

(50) Fritzinger, B.; Capek, R. K.; Lambert, K.; Martins, J. C.; Hens, Z. *J. Am. Chem. Soc.* **2010**, *132*, 10195.
(51) Frederick, M. T.; Achtyl, J. L.; Knowles, K. E.; Weiss, E. A.; Geiger, F. *J. Am. Chem. Soc.* **2011**, *133*, 7476.
(52) Choi, J.-H.; Fafarman, A. T.; Oh, S. J.; Ko, D.-K.; Kim, D. K.; Diroll, B. T.; Muramoto, S.; FGillen, J. G.; Murray, C. B.; Kagan, C. R. *Nano Lett.* **2012**, *12*, 2631.
(53) Kiedron, P. W. *Proceedings of the Eleventh Atmospheric Radiation Measurement (ARM) Science Team Meeting*, Atlanta, GA, March 2001.
(54) Boivin, M.; Lamarre, S.; Tessier, J.; Lecavalier, M.-E.; Najari, A.; Dufour-Beausejour, S.; Dussault, E. B.; Collin, P.; Allen, C. *Appl. Phys. Lett.* **2012**, *100*, No. 033302.